Web: www.witpress.com Email witpress@witpress.com
Paper from: *Advanced Computational Methods in Heat Transfer*, B Sunden and CA Brebbia (Editors).
ISBN 1-85312-906-2

TB dynamic behaviour during thermal shocks - simulation and experiment

Z. Veselý[1], J. Kuneš[1], M. Honner[1], J. Martan[2]
[1]*New Technologies Research Center, University of West Bohemia, Czech Republic.*
[2]*Department of Physics, University of West Bohemia, Czech Republic.*

Abstract

Thermal barriers (TB) protect material against high temperatures and thermal shocks. The effect of various TB - substrate structures to their dynamic behaviour under the thermal shock is studied. The TB parameters such as number of individual layers, their thicknesses and porosities and thermal and mechanical properties of their materials have been investigated. Temperature measurement on the experimental samples has been done both during the plasma spraying and thermal loading. Indirect thermal problems have been solved to determine the effect of TB's. The simulation model has been compared with the temperature measurement on selected TB's structures. Simple model in the form of criterial equation has been constructed in order to control the TB deposition process. The presented results confirm the importance of TB's as a dynamic material protection against the thermal overloading.

1 Introduction

Thermal barriers (TB) protect material of machine parts against high temperatures and thermal shocks. Their importance increases with the orientation to more powerful and economical energy appliances and further in recent advanced manufacturing technologies. The objective of this paper is to present our current research on the TB's.

Paper from: *Advanced Computational Methods in Heat Transfer*, B Sunden and CA Brebbia (Editors).
ISBN 1-85312-906-2

1.1 TB advantages

TB's usually represent a heterogeneous multilayer coating deposited on the surface of thermal loaded machine parts those temperature should be decreased. Potential advantages of thermal barriers can be summarized into following:
1) Keeping the protected machine part surface at the same value, the appliance operation temperature can be increased along with the increase of the TB thickness, that means the higher appliance efficiency.
2) On the other hand, using the TB protected machine part along with keeping the appliance operation temperature at the same value, it leads to the decrease of substrate surface temperature that means the increase of machine part operation lifetime.

1.2 TB physical structure

The TB structure is given by the technological and operational requirements. TB's usually consist of the top ceramic layer, additional layer and bond coat. Thermal and mechanical properties of these layers are essentially different. It considerably affects the dynamics of thermal and especially thermally induced stress processes.

The top ceramic layer, usually ZrO_2, must have high thermal resistivity, sufficient reflectance for infra-red radiation and must satisfy stress and strain conditions. The bond coat must offer fair tolerance against high temperature corrosion and oxidation. Further, the bond coat helps binding the ceramic layer to the substrate and helps accommodating the mechanical deformation caused by different coefficients of thermal expansion and modulus of elasticity for the ceramic layer and the substrate. The additional layer, made of Al_2O_3, represents a diffusion barrier that decreases an oxidation of the bond coat and the underlaying substrate.

The detailed information about the TB physical structure, production, test performance, lifetime modelling, etc. can be found in a relatively numerous literature, e.g. in [1], [2] and [3].

1.3 TB material properties

The TB - substrate structure represents a nonlinear heterogeneous thermomechanical system. It is important to obtain the sufficiently accurate thermal and mechanical properties of individual TB and substrate materials. Inaccuracy of these material parameters significantly affects the results of a numerical solution, particularly when the dynamic TB behaviour is analyzed.

Following these arguments, the detailed analysis of thermal and mechanical properties have been made. The available published experimental data have been collected and analytical temperature dependence of the individual material properties has been proposed. Analytical functions of thermal and mechanical properties for ZrO_2, Al_2O_3, Nimonic 90 and substrate materials are in [4] and [5].

Paper from: *Advanced Computational Methods in Heat Transfer*, B Sunden and CA Brebbia (Editors).
ISBN 1-85312-906-2

2 Simulation

During the operation conditions the machine parts of high temperature appliances are subjected to various modes of damage including the difference between the thermal expansion coefficients of layers, phase transformations within the ZrO_2, erosion, oxidation and high temperature corrosion by molten salts. TB's should be tolerant to these failure modes and should stay well bonded to the substrate during the requested lifetime.

It is impossible to include all of these complicated processes to the computer simulation. The reaction of the TB - substrate structure only at the beginning short time period after the thermal shock on the TB surface is investigated here. Therefore, the processes that are important during long term cyclic thermal loading such as phase transformation within ZrO_2, oxidation, high temperature corrosion by molten salts, etc. are not taken into account. Only the thermomechanical process (heat transfer and thermally induced stress and strain with the consideration of the elastic mechanical properties) is simulated within the TB - substrate structure. Detailed information about mathematical model of thermal and thermal stress problems can be found in [4] and [5].

The computational system MARC implements transformation of the problem to the computational model utilizing the finite element method.

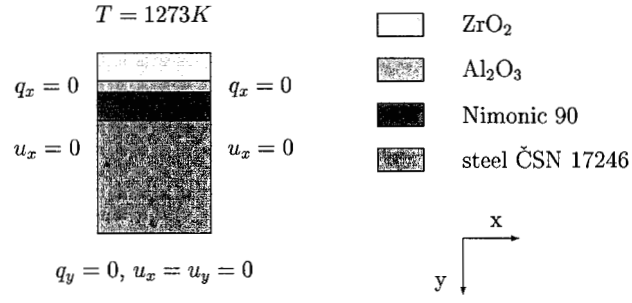

Figure 1: Geometry and boundary conditions of the model

The planar geometry and boundary conditions are plotted in Fig. 1. Zero stress and the temperature of 293 K in the whole TB - substrate structure have been taken as the initial conditions.

The effect of the time and space steps on the simulations results are in [4] and [5]. The results of the simulations are presented in [5], [6] and [7]. The mutual comparisons of raw substrate, one -, two - and three - layer TB structures are discussed in [4].

Fig. 2 illustrates three-layer TB structure thickness comparison. The solid lines represent temperature development and the dotted lines represent thermal stress development. Individual time levels 0.2, 1, 4 and 10 s are indicated by symbols.

Paper from: *Advanced Computational Methods in Heat Transfer*, B Sunden and CA Brebbia (Editors).
ISBN 1-85312-906-2

Fig. 2 clearly shows the effect of individual layer thickness increase. The ZrO_2 layer thickness modification has the largest influence on the monitored quantities. The lower the time level is, the larger the influence is due to the TB dynamic protection against thermal overloading.

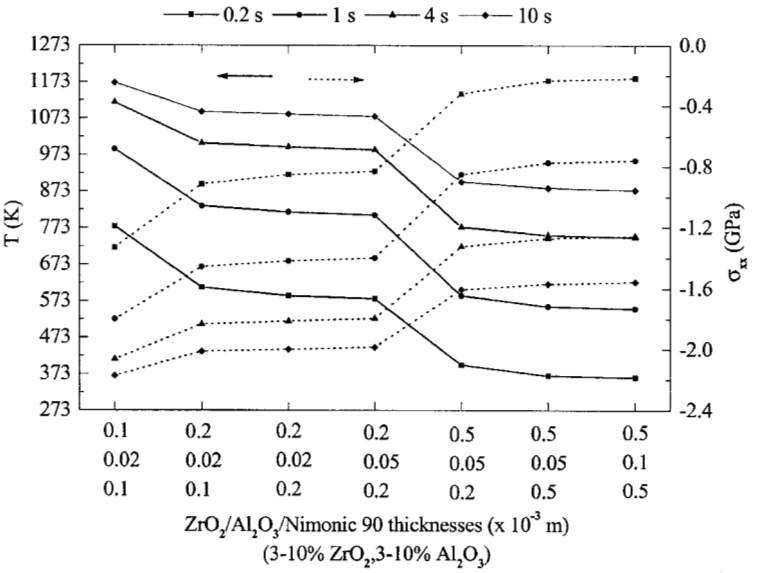

Figure 2: Three-layer TB structures - T, σ_{xx} as a functions of layer thicknesses

3 Experiment

3.1 Plasma deposition of TB samples

The substrate samples with the dimension 100 x 70 x 20 mm have been made (steel DIN X10CrNiTi18.10, ČSN 17 246). Total number of 8 holes with 0.6 mm diameter have been drilled from the back side of the sample to various depth from the sample front side, so the substrate surface remained undisturbed. Each sample includes 6 measurement positions inside the sample (from 1.5 to 4 mm under the substrate surface), one position for measurement of substrate surface temperature and one position for temperature measurement above the substrate. The sample front side with the TB layer and sample backside with the embedded thermocouples are shown on Fig. 3. The coated Ni - NiCr thermocouples with 0.5 mm diameter have been used. The thermocouples at the substrate surface and 1 mm above substrate surface have been embedded to the sample after the sample surface grit blasting in order to avoid their damage.

The individual TB layers have been deposited by air plasma spraying process using the prototype Eutronic Plasma device manufactured by Eutectic + Castolin Institute. Resultant TB samples consisted of only two

Paper from: *Advanced Computational Methods in Heat Transfer*, B Sunden and CA Brebbia (Editors).
ISBN 1-85312-906-2

layers - bond coat and top ceramic layer. The TAFA powder NiCoCrAlY has been used for the bond coat and TAFA powder ZrO_2 - 7.5% Y_2O_3 (or optionally POREXI powder Al_2O_3 - 3% TiO_2) have been used for the ceramic layer. The following deposition parameters current 630 A, voltage 62 V, Ar flow 60 $l.min^{-1}$, H_2 flow 8.49 $l.min^{-1}$, powder carrying Ar flow 1.79 $l.min^{-1}$ and powder carrying Ar pressure 0.45 bar have been set to NiCoCrAlY deposition; current 550 A, voltage 60 V, Ar flow 41 $l.min^{-1}$, H_2 flow 9.99 $l.min^{-1}$, powder carrying Ar flow 2.49 $l.min^{-1}$ and powder carrying Ar pressure 0.55 bar have been set to ZrO_2 - Y_2O_3 deposition and current 630 A, voltage 62 V, Ar flow 45 $l.min^{-1}$, H_2 flow 11.99 $l.min^{-1}$, powder carrying Ar flow 2.99 $l.min^{-1}$ and powder carrying Ar pressure 0.40 bar have been set to Al_2O_3 - TiO_2 deposition.

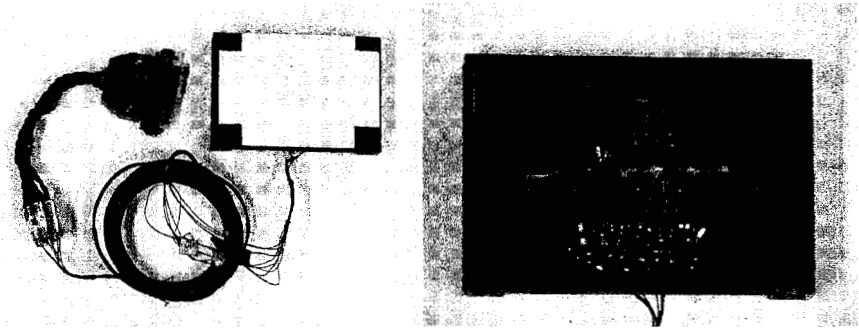

Figure 3: The sample III with the deposited TB (left) and detail of the sample back side with the embedded thermocouples (right)

Plasma sprayer velocity of 2 $m.min^{-1}$ has been used and the torch - sample distance has been set to 110 mm. The sprayer passed over the sample in the horizontal direction with the vertical spacing of 15 mm during the bond coat deposition. The vertical spacing of 5 mm has been used during ZrO_2 - Y_2O_3 layer deposition and of 10 mm during Al_2O_3 - TiO_2 deposition. The vertical spacings of the sprayer passes have been determined in order to achieve the layers with the best homogeneity in the layer surface profile.

The individual layer thickness has been monitored. The sample surface profile has been measured in three longitudinal and three lateral directions on the as-prepared sample, after the grit blasting and after the deposition of each TB layer. The presented sample III (substrate/NiCoCrAlY/ZrO_2-Y_2O_3) has average TB layer thicknesses 160 μm NiCoCrAlY and 195 μm ZrO_2 - Y_2O_3. The temperature evolution has been measured during the plasma spraying to monitor the effect heat transfer on the layer's deposition.

The apparent and skeletal density of ZrO_2 - Y_2O_3 and Al_2O_3 - TiO_2 layers have been measured by the He - pycnometry method (AutoPycnometer 1320 device fy. Micromeritics USA) and the pore distribution curve by the Hg - porosimetry method (AutoPore 9200 device fy. Micromeritics USA). The measured data are arranged in the Tab. 1. Both materials have

Paper from: *Advanced Computational Methods in Heat Transfer*, B Sunden and CA Brebbia (Editors).
ISBN 1-85312-906-2

monodispersive pore structure with the median pore diameter given in the Tab. 1.

Table 1: Porosity data

TB layer	ZrO_2 - Y_2O_3	Al_2O_3 - TiO_2
median pore diameter (nm)	999.3	1084.4
total pore area ($m^2.g^{-1}$)	0.282	0.270
porosity (%)	18.5	18

3.2 Thermal loading of TB samples

The TB samples have been thermal loaded by oxygen - acetylen flame. The C_2H_2 pressure 0.5 bar, O_2 pressure 2.5 bar, air pressure 1.5 bar, torch - sample distance 120 mm and torch velocity 3.0 $m.min^{-1}$ have been used. The torch cyclically passed over the sample in the center horizontal plane. Dead point of the cycle has been 50 mm from the sample edge. The number of 40 cycles have been used. The sample temperatures exceeded 1000 K. The processes of sample thermal loading have been monitored by digital infra-red camera Thermacam SC2000 fy. FLIR System and digital video camera. The recorded data have been used for the analysis of sample surface temperature distribution during the torch motion. Fig. 4 shows the torch moving across the sample in visible and infra-red spectras.

Figure 4: Thermal loading in visible and infra-red spectras

Temperatures inside the sample have been measured by the built-in thermocouples. The thermocouples 1–3,5,7 and 8 were in the center horizontal plane of the sample in various depths from the surface. The thermocouple 4 has been 15 mm above the center horizontal plane 1 mm above the sample surface. And finally thermocouple 6 has been 7.5 mm under the center horizontal plane at the TB - substrate interface. The temperatures measured during the sample III thermal loading are in Fig. 5.

Samples have been thermal loaded by cyclic passing of the torch over the surface. The part of the time period of the cycle the torch moves over the sample surface (heating time) and the rest of the cycle the torch moves

Paper from: *Advanced Computational Methods in Heat Transfer*, B Sunden and CA Brebbia (Editors).
ISBN 1-85312-906-2

from the sample to the dead points of the cycle (cooling time). The cooling time can be seen on the Fig. 5 when the temperatures above the surface are lower than the temperatures inside the sample.

The ratio of heating and cooling times during the cycle causes the situation that after the certain number of cycles, the temperatures inside the sample with TB reached higher values than in the sample without TB. Similarly, the temperatures inside the sample with TB having a better thermal performance reached higher values than in the sample with low thermal performance TB. The higher performance TB better protect the sample during heating time but equally prevent the sample front side cooling during the cooling time.

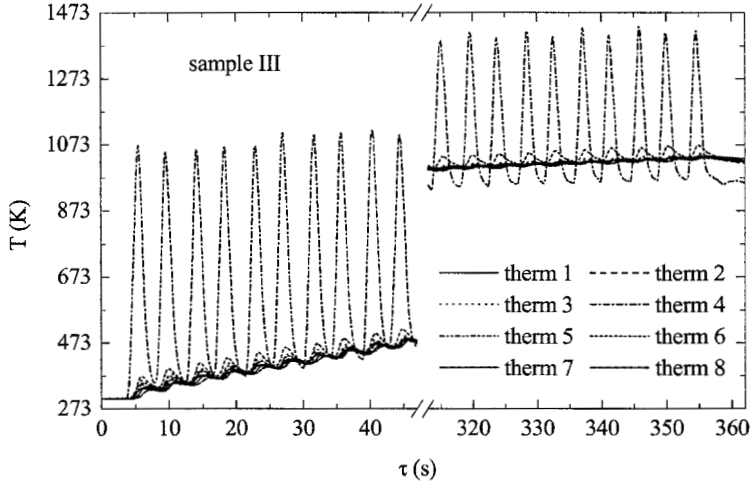

Figure 5: Temperature distribution during the sample III thermal loading

The distance from the dead point of the cycle to the sample edge influences the ratio of the heating and cooling times and finally affects the heating process. The effect of the dead point distance from the sample edge is going to be studied.

4 Measurement and simulation comparison

4.1 Heat transfer comparison

The simulation model [8] solves the indirect problem of determination of heat flux intensities on the surface of the coated material. The effect of a moving torch is expressed as a time and space dependent boundary condition prescribing heat fluxes on the substrate surface. Heat transfer intensity from the torch to the coated material is realized dependent on the radial distance from the axis of the torch. In conjuction with a trajectory of the torch in the form of x, y, z and t coordinates it defines space and time dependent boundary conditions.

Paper from: *Advanced Computational Methods in Heat Transfer*, B Sunden and CA Brebbia (Editors).
ISBN 1-85312-906-2

The sample surface heating by the torch and radiation losses from the surface to the ambient through the surrounding hot fluid during the thermal loading process are assumed.

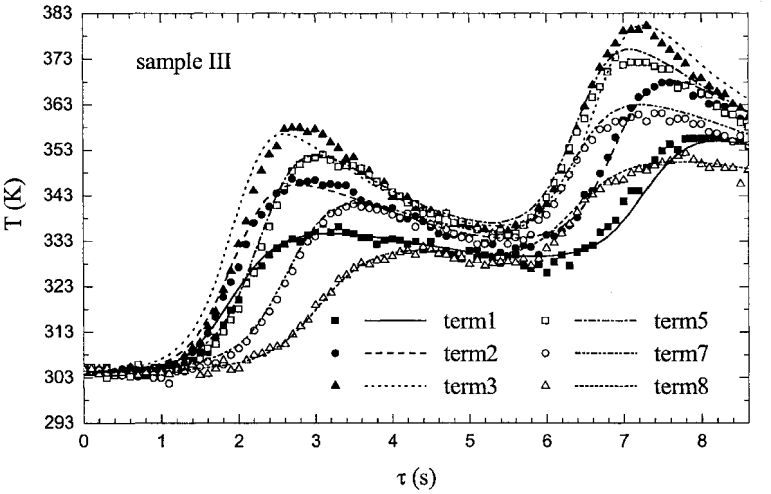

Figure 6: Measured and computed temperatures during the sample III thermal loading

Heat conduction in a 2D substrate geometry along the trajectory of the torch in the sample center horizontal plane is calculated using the finite element method by the Cosmos/M software. The front side sample surface is subjected to the thermal loading and the remaining lateral sides and back side of the sample are assumed insulated as the simulation is performed for only the first loading cycle. The time dependent loads at the front side sample surface are precalculated, being different for each surface element of the discretization grid. Then temperatures inside the sample are calculated. The time evolution in the nodes corresponding with the position of thermocouples are compared with the measured values. The parameters of the model have been iteratively fitted to match the experimental results measured by thermocouples. This was achieved by adusting the curve of the heat transfer coefficient over the radial distance from the axis of the torch. The trajectory of the torch in time had to be assigned in accordance with experiments as well.

The distribution of the heat transfer coefficient over the radial distance from the torch axis has been found and fitted in the model of raw substrate without TB. Then the models of the samples with TB have been created. The model of the TB sample has the same geometry as the sample without TB, e.g. the TB layer is not included in the TB sample model and the effect of TB is simulated as the change of the heat transfer coefficient distribution.

The heat transfer coefficient distribution corresponding to the sample III has been find to be the 90 % of the heat transfer coefficient identified to fit the thermal loading of the sample without TB.

Paper from: *Advanced Computational Methods in Heat Transfer*, B Sunden and CA Brebbia (Editors).
ISBN 1-85312-906-2

Fig. 6. illustrates the comparison of measured and computed values of the temperature in the sample III. The first pass of the torch over the sample shows a good agreement between the measured and computed data. The second pass (the second half of the first cycle) indicates that computed temperatures are some higher than the measured ones. This effect is caused by the 2D model geometry.

The 3D simulation model involving the heat transfer from the back and lateral sides of the sample is being prepared in order to simulate the full thermal loading process.

4.2 Deposition process model

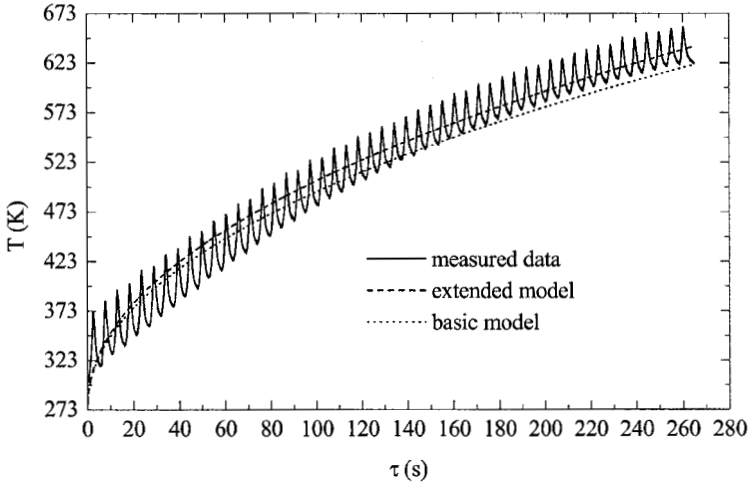

Figure 7: Measured and criterial equation model data

The presented model has been developed to describe the deposition process of the TB's. Development of the precise mathematical model of plasma spraying and subsequent thermal transfer to the sample is a rather complicated task. The more simple criterial equation model enables prediction of the sample substrate temperature from the knowledge of the spraying process and material parameters. The physical analysis of the spraying process have been conducted. Having a number of experimental data of various TB deposition processes, the proposed basic equation has been developed and extended to include all the important process parameters. The resultant extended criterial equation for dimensionless substrate surface temperature Θ_s

$$\Theta_s = 0.0851 Fo^{0.4742} Ki^{-1.8318} K_1^{-0.1960} M_{Ar}^{-0.6882} M_{H2}^{-0.9647} \Theta_{ini}^{-2.8516} \qquad (1)$$

consists of the Fo criterium (representing dimensionless time variable), Ki criterium (rep. thermal flux to the substrate), K_1 criterium (rep. the torch motion), M_{Ar}, M_{H2} (rep. mass flux of Ar and H_2 gases) and Θ_{ini} criterium (rep. the initial temperature distribution). The Fig. 7 illustrates the criterial equation model compared to the measured substrate surface thermocouple data during the simulation of the bond coat deposition.

Paper from: *Advanced Computational Methods in Heat Transfer*, B Sunden and CA Brebbia (Editors).
ISBN 1-85312-906-2

5 Conclusions

The simulation model of the TB sample has been created. Dynamic protection of various TB structures against thermal overloading has been compared. Several TB structures were deposited onto steel samples with embedded thermocouples. Temperatures were measured both during the TB deposition and thermal loading of the samples. The experimentally obtained temperature evolutions at various depths and locations in the samples were used to find the heat transfer intensity to the surface during thermal loading. The criterial equation deposition process model was developed to predict the sample substrate temperature from the knowledge of the deposition process and material parameters. The importance of TB's as a dynamic material protection against thermal overloading has been confirmed.

Acknowledgement

The work has been done within the framework of the R&D project No. LN00B084 supported by the subvention of the Ministry of Education, Youth and Sports of Czech Republic.

References

[1] Bengtsson, P. & Persson, Ch., Modelled and measured residual stresses in plasma sprayed thermal barrier coatings, *Surface & Coatings Technology*, **92**, pp. 78–86, 1997.

[2] Brindley, W. J., Properties of plasma-sprayed bond coats, *Journal of Thermal Spray Technology*, **6(1)**, pp. 85–90, 1997.

[3] Schmitt–Thomas, Kh. G. & Dietl, U., Thermal barrier coatings with improved oxidation resistance, *Surface and Coatings Technology*, **68/69**, pp. 113–115, 1994.

[4] Kuneš, J. & Veselý, Z., Numerical simulation of thermal barrier dynamic behaviour during thermal shocks, *Industrial Heat Engineering*, **23(4)**, 2001

[5] Kuneš, J. & Veselý, Z., Numerical solution of the thermomechanical proceses in the thin layer structure of thermal barrier, *Computer Assisted Mechanics and Engineering Sciences*, **7**, pp. 207–218, 2000.

[6] Veselý, Z., The effect of TB structure on the thermomechanical process in the material, *Proc. of the Int. Conference on Material Science on the Threshold of 3rd Milenium,* Vysoké učení technické v Brně, Czech Republic, pp. 70-74, 1999.

[7] Kuneš, J. & Veselý, Z., Numerical solution of the thermomechanical processes in the thin layer structure of thermal barrier, *Proc. of the VII. Int. Conference on Numerical Methods in Continuum Mechanics,* eds. Kompiš, V. Žmindák, M., Hučko, B., University of Žilina, Slovak Republic, pp. 259–264, 1998.

[8] Honner, M., Červený, P., Franta, V., Čejka, F., Heat transfer during HVOF deposition, *Surface & Coatings Technology,* **106**, pp. 94–99, 1998